Received: Added at production | Revised: Added at production | Accepted: Added at production

DOI: xxx/xxxx

ARTICLE TYPE

Using model error in response history analysis to evaluate component calibration methods

Adam Zsarnóczay* | Jack W. Baker

[1]Department of Civil & Environmental Engineering, Stanford University, California, USA

Correspondence
*Adam Zsarnóczay,
Email: adamzs@stanford.edu

Abstract

This research is part of a larger effort to better understand and quantify the epistemic model uncertainty in dynamic response-history simulations. This paper focuses on how calibration methods influence model uncertainty. Structural models in earthquake engineering are typically built up from independently calibrated component models. During component calibration, engineers often use experimental component response under quasi-static loading to find parameters that minimize the error in structural response under dynamic loading. Since the calibration and the simulation environments are different, if a calibration method wants to provide optimal parameters for simulation, it has to focus on features of the component response that are important from the perspective of global structural behavior. Relevance describes how efficiently a calibration method can focus on such important features. A framework of virtual experiments and a methodology is proposed to evaluate the influence of calibration relevance on model error in simulations. The evaluation is demonstrated through a case study with Buckling Restrained Braced Frames. Two calibration methods are compared in the case study. The first, highly relevant calibration method is based on stiffness and hardening characteristics of braces; the second, less relevant calibration method is based on the axial force response of braces. The highly relevant calibration method consistently identified the preferable parameter sets. In contrast, the less relevant calibration method showed poor to mediocre performance. The framework and methodology presented here are not limited to BRBF. They have the potential to facilitate and systematize the improvement of component-model calibration methods for any structural system.

KEYWORDS:
model uncertainty; calibration method; calibration error; calibration relevance; buckling restrained braced frames

1 | INTRODUCTION

Simulation of dynamic structural response to seismic excitation is becoming common in research and engineering practice. Performance-based design is quickly gaining popularity among practicing engineers[1,2], and several components of modern seismic guidelines are based on extensive simulations of the behavior of various structural systems[3]. In spite of their widespread use, the accuracy of dynamic response-history simulations (i.e., the uncertainty in simulated structural response) is poorly

understood. This stems from the complexity and the significant variance associated with seismic excitation as well as the scarcity of available reference data that could be used to assess the accuracy of simulation results.

The long-term objective of this research is to better understand and quantify the epistemic uncertainty in the models (i.e., the uncertainty that stems from having imperfect models) that are used in dynamic response-history simulations. We will refer to such uncertainty as *model uncertainty* in this paper. If model uncertainty is quantified, it will be possible to consider it implicitly in the simulations - similarly to contemporary efforts to quantify the uncertainty of structural geometric and material properties by using random variables as corresponding inputs.

Defining model uncertainty is the first step towards its quantification. This task is difficult because direct measurement of dynamic simulation accuracy is typically not possible. In the prevalent multi-level modeling approach, the structural model of a building is made up from component models (e.g., uniaxial brace models, plastic hinge models for beam-column connections) that are calibrated independently from each other using component-specific laboratory test results. The quality of individual component models (i.e., their ability to reproduce laboratory tests) is often assumed to be a good proxy for the quality of the component-model assembly. Best-fit component models are assumed to be perfect and the potential bias due to model imperfection is assumed to be negligible in contemporary research (e.g., Ibarra and Krawinkler[4], Kwon and Elnashai[5], Padgett and DesRoches[6], Dolsek[7], Liel et al.[8], Kazantzi, Vamvatsikos, and Lignos[9], Gokkaya, Baker, and Deierlein[10], O'Reilly and Sullivan[11]).

We present a framework in this paper that uses virtual experiments to evaluate component-model calibration methods based on the performance of calibrated component-model assemblies. We focus on understanding what makes a component calibration method desirable and how various calibration methods can be compared to each other. The results highlight problems with current calibration practice. The presented framework can be used to discover novel calibration approaches that lead to more accurate response simulations and provide a measure of expected error due to imperfect models.

1.1 | Background

The input data and the methodology of dynamic response-history simulations are heavily affected by several sources of uncertainty. Consequently, structural response is characterized probabilistically and design objectives account for this variability[2]. Such a Probabilistic Seismic Performance Assessment (PSPA) framework shall consider all major sources of uncertainty and their influence on the structural response. The uncertainty in simulated structural response stems from uncertainty in inputs, and uncertainty in models[12].

PSPA inputs, such as ground motion records as dynamic loads, material properties of the structural components, and the geometry and layout of the structure, are all observable. Their uncertainty can be quantified using empirical data. This type of uncertainty is routinely recognized in contemporary PSPA by considering inputs as random variables and propagating their uncertainty through every step of the analysis[9].

PSPA uses structural and probabilistic models. The structural model describes the structural response as a function of the analysis inputs. The probabilistic model describes the distributions of the random variables and the dependencies between them throughout the analysis. Both types of models are mathematical idealizations of reality. They employ simplifications for the sake of efficiency and they are formulated based on a finite number of experimental observations. A structural model, for example, might simulate the response of a two-dimensional braced frame to represent the seismic response of a three-dimensional building. A probabilistic model might use a multivariate normal distribution with a simple correlation structure to characterize the uncertainty in structural material parameters. Although the imperfection of these models might introduce significant error in the simulated structural response[13], they receive less attention in PSPA-related literature.

Uncertainty due to the imperfection of models is typically combined with uncertainty in the inputs that describe structural properties under the umbrella of model uncertainty. The influence of model uncertainty is considered either by increasing the variance of inputs, or by increasing the variance of simulated structural response during post-processing[14]. Such an approach assumes that the models are unbiased and that their error is independent of the input parameters (including the ground motions). We are not aware of studies from the literature that support such assumptions in the context of PSPA. Results of several recent blind-prediction contests suggest that structural models can be biased and the error in simulated structural response can be significantly larger than expected[15,16].

The problem of poorly understood model uncertainty is exacerbated by the sparsity of reference data on dynamic structural response. Performing a sufficiently large number of full-scale dynamic experiments for calibration purposes is prohibitively expensive. Data from structural health monitoring systems is a cheaper alternative[17,18]. When a dynamic response-history and

an almost-perfect Finite Element Model (FEM) are available, recent developments in FEM updating [19,20] enable estimation of model parameters with sufficient accuracy. However, such data is only available for existing buildings and each building can provide at most one response-history that corresponds to significant damage or collapse.

In most practical applications, the FEM is imperfect. Errors in model geometry, masses, and the mathematical model for material behavior had been shown to make calibration more challenging and significantly increase the magnitude of error in parameters and simulated response [21]. Consequently, instead of direct calibration to dynamic structural response, engineers often rely on a multi-level modeling approach. They identify key components of the structure and calibrate corresponding sub-models, referred to as component models, using smaller-scale, less expensive, often quasi-static experiments. These component-specific experiments are expected to improve component models, and those improvements shall lead to better structural response estimates. We argue that such improvements are not trivial, and their extent heavily depends on how the component model is calibrated.

1.2 | Problem statement

The multi-level modeling approach introduces error and corresponding uncertainty in the structural model. Figure 1 illustrates a typical series of transformations that connect the dynamic structural response of interest with the quasi-static component response used for calibration. The following environments are depicted in the figure:

I Structural response under dynamic excitation. The simulation uses the complete structural model and a ground motion record to estimate the real response of the reference structure under seismic excitation.

II Component response under equivalent dynamic loading. The simulation uses a component model coupled with a mass and an equivalent acceleration history to estimate the response of a component in the reference structure under seismic excitation.

III Component response under equivalent quasi-static loading. The simulation uses a component model and an equivalent displacement history to estimate the response of a component in the reference structure under seismic excitation.

IV Component response under standardized quasi-static loading. The simulation uses a standardized displacement history to evaluate the component model by comparing the results of experiments to those of the simulation. This is typically the only environment where experimental results are available.

Potentially important information about the structural model is lost in each transformation. In moving from environment I to II, by focusing on a single component, engineers lose the information about the interaction between components. The next transformation to environment III changes the control from dynamic acceleration to quasi-static displacement. The sample response demonstrates how that transformation affects the observed error in the simulation. The final transformation to environment IV modifies the prescribed deformation-history. This might change the energy-dissipation and inelastic-deformation demands significantly.

When calibrating the component model in environment IV in Figure 1, engineers shall focus on the features of the component model that are relevant to the dynamic structural response (environment I) that they aim to simulate. *Calibration relevance* in this paper refers to the capacity of the calibration method to focus on such relevant features of the structural model. A set of component-model parameters that seems to provide reliable results (i.e., simulates experimental response in environment IV with small error) might still lead to significant error in dynamic simulations if the calibration lacks relevance. An illustrative example of such a case is the calibration of a cyclic-hardening structural component using only monotonic experiments. Monotonic experiments lack relevance because they do not inform us about the cyclic behavior of the component.

Although real, quasi-static calibration environments are typically more relevant than the one in the previous example, the structural model and the calibration method can never be perfect. The resulting inaccuracy of the calibrated model is already recognized in the broader engineering literature [22,23]. Model calibration in structural engineering is often focused on reducing the error in simulations of the quasi-static component tests. This is conceptually identical to assuming perfectly relevant calibration, and simplifying the problem to the maximization of model reliability within the environment used for calibration. The assumption of perfect relevance seems to be a hypothesis carried over from earlier calibration efforts, such as investigation of column buckling, where the simulated phenomenon was directly observable in quasi-static experiments. We are not aware of any studies of the applicability of such assumptions for the dynamic response simulations in PSPA.

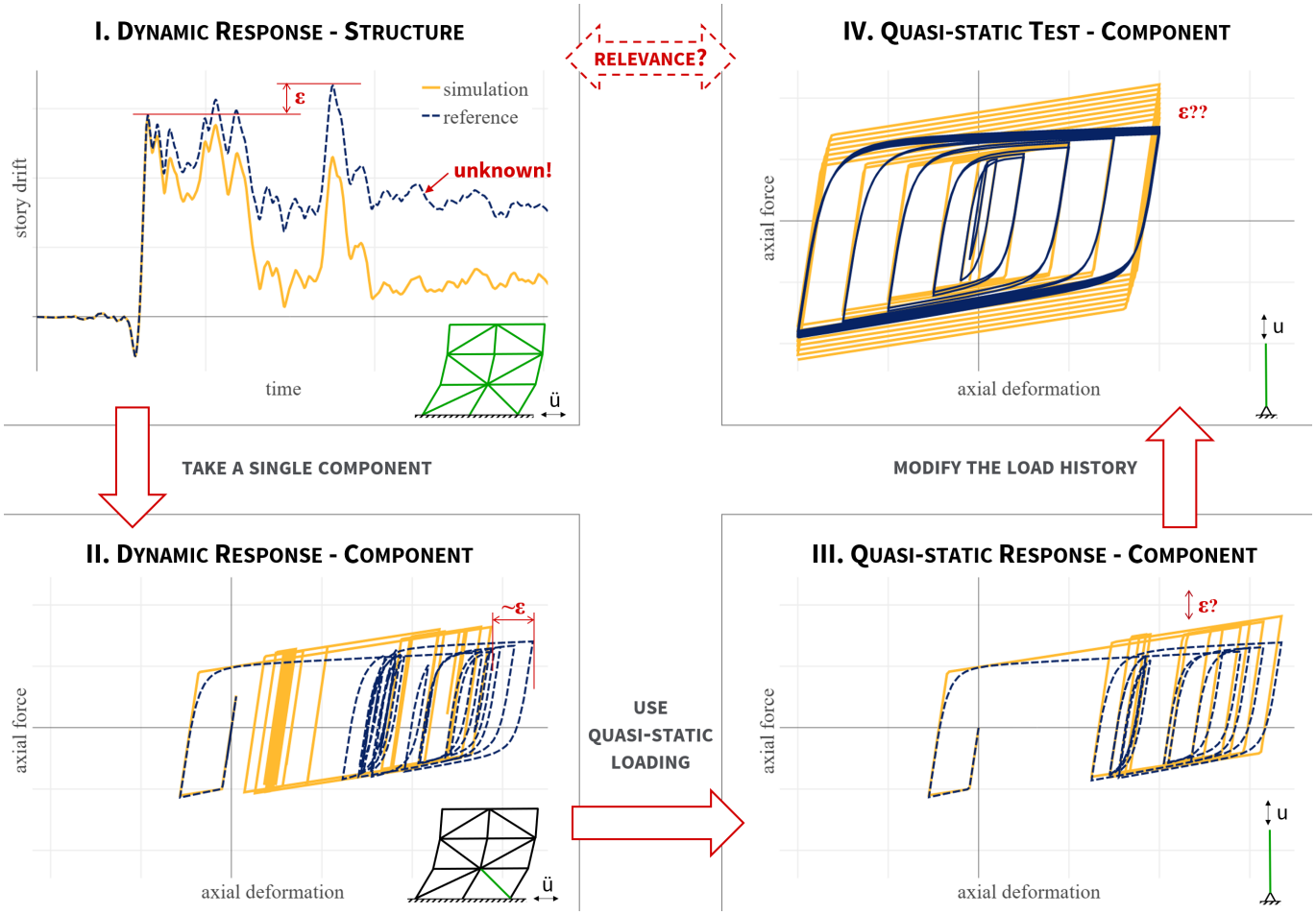

FIGURE 1 The three typical transformations that connect real dynamic response of a structure to the quasi-static response of its primary component in laboratory tests. The definition of error (ε) in IV is not trivial and it has a significant influence on the relevance of the calibration.

Calibration in more relevant environments is typically more challenging and leads to a reduction in perceived model reliability[22]. Consequently, if relevance is taken into consideration, calibration becomes an optimization problem with conflicting objectives presented by relevance and reliability. Solution of this optimization problem requires quantitative information about the error in dynamic simulations conditioned on various levels of model reliability and calibration relevance.

Real, full-scale, dynamic experiments on structures are expensive, time consuming, and not perfectly reproducible. Their quantitative evaluation is hindered by the small sample size and the inevitable additional uncertainty due to imperfect specimens and measurement errors. The lack of experimental data for high-level models (i.e., realistic, global structural models from environment I) in structural engineering makes it practically impossible to evaluate calibration relevance through a direct comparison of simulated and real structural response.

The following sections present a framework of virtual experiments that we can use to improve our understanding about calibration relevance and identify efficient calibration methods. We use a state-of-the-art, high-fidelity model to represent the real behavior of a structural system, and a simplified, low-fidelity model to represent an imperfect simulation model of the same system. Since both models are numerical, virtual experiments allow us to compare their quasi-static and dynamic responses and investigate the importance of calibration relevance in the multi-level modeling environment illustrated in Figure 1.

2 | OBJECTIVES AND SCOPE

We worked towards four objectives to investigate how simulated dynamic response is affected by the relevance of the calibration method:

1. Develop a framework of virtual experiments that reproduces important features of realistic component model calibration and allows engineers to rank calibration methods by their efficiency in minimizing the error in simulated dynamic structural response.
2. Evaluate the efficiency of a typical calibration method.
3. Propose modifications to the typical calibration method introduced earlier that are expected to improve its relevance.
4. Evaluate the efficiency of the modified calibration method, and compare the two calibration methods.

We chose Buckling Restrained Braced Frames[24] (BRBF) as a vehicle to introduce and evaluate the proposed methodology. The diagonal Buckling Restrained Braces (BRBs) of such frames are well-known for their stable, hardening behavior under cyclic loading[25,26]. All inputs (e.g., structural geometry, material properties) of the dynamic simulations are considered deterministic with the exception of the set of ground motion records that describe the seismic hazard. This simplification significantly reduces the computational demand of the dynamic simulations without affecting qualitative observations about model uncertainty. We used a large and diverse set of ground motions to be able to investigate the relationship between record-to-record (RTR) and model uncertainty.

3 | CALIBRATION METHODS

Before discussing details of the framework of virtual experiments, we define two calibration methods below that will serve as examples later. The framework presented afterward is not limited to these methods. They were selected to provide insight on the advantages of using information beyond the raw test data to calibrate component models. The two calibration methods can be summarized as follows:

1. Minimize the error in the simulated forces over the force-deformation response. This method will be referred to as *force-based* for brevity.
2. Minimize the error in the inelastic stiffness and the cyclic hardening of the component. Those features can be inferred from force-deformation data. This method will be referred to as *stiffness-hardening-based* for brevity.

The mathematical model for calibration is defined as the minimization of a calibration error function $\varepsilon_{CAL}(r, s)$ that is proportional to the difference between the reference (r) and the simulated (s) behavior. The error function might have several components to combine the influence of errors in multiple important features. The reference behavior is only influenced by the characteristics of the tests, while the simulated behavior also depends on the type of component model used and the parameters set for that model. An ideal calibration method has an error function that is not sensitive to r; i.e., it can be used to identify high-quality component models within a wide range of load histories and specimens. Note: the quality of a component model depends on the error in dynamic response simulations while the calibration error associated with the component model is based on quasi-static component response.

3.1 | Force-based method

Following common calibration practice (e.g., Black, Makris, and Aiken[27], Zona and Dall'Asta[28]), the force-based calibration error $\varepsilon_{\mathrm{CAL,F}}(r, s)$ is defined as the root-mean-squared difference between quasi-static force responses:

$$\varepsilon_{\mathrm{CAL,F}} = \sqrt{\frac{1}{n}\sum_{i=1}^{n}(F_{s,i} - F_{r,i})^2} \tag{1}$$

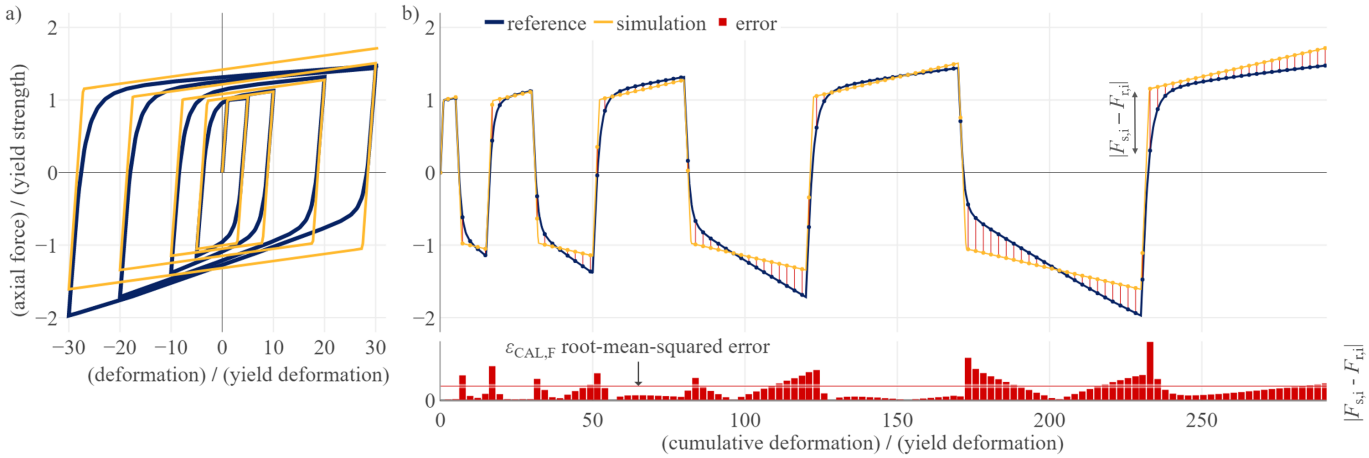

FIGURE 2 Calculation of the force-based calibration error: a) force-deformation plot of the reference and the simulated cyclic response; b) force responses as a function of cumulative deformation with the error measure and $\varepsilon_{\text{CAL,F}}$ highlighted

where $F_{s,i}$ and $F_{r,i}$ are the i^{th} simulated and reference (i.e., measured) force response data points, respectively; n is the total number of data points used for the calibration. Figure 2 illustrates the calculation of $\varepsilon_{\text{CAL,F}}$ using results from virtual experiments. The reference result is generated with a complex nonlinear BRB component model. The simulation results use a component model that is limited to a bilinear hardening behavior. Details on both models are provided later in the paper.

The force-based method assumes that the errors in dynamic response simulation are proportional to $\varepsilon_{\text{CAL,F}}$, hence minimizing that quantity will help engineers select an optimal component model for dynamic analysis. There are several problems with this assumption:

- Forces are poor proxies for dynamic response of components that exhibit inelastic behavior. Dynamic response of such components is better described by their deformation or stiffness.
- All $(F_{s,i} - F_{r,i})$ samples have identical weight. This suggests that every data point from the test is equally important. It would be easy to argue for different weights in the elastic and inelastic parts of component response in Figure 2.
- The quadratic error function that yields $\varepsilon_{\text{CAL,F}}$ is heavily affected by outliers, such as the error at 233 normalized deformation in Figure 2b. That particular error is due to the lack of smooth transition from elastic to inelastic behavior in the component model. There are other, more important issues described in the next section that the force-based error function does not recognize.
- The quadratic error function is symmetric: errors in either direction will have the same contribution to $\varepsilon_{\text{CAL,F}}$. Overestimating the force-response of a component is unlikely to result in errors of the same magnitude in dynamic simulation than underestimating them.

These problems - which are applicable to typical component calibration exercises - significantly reduce the likelihood that the force-based method can identify high-quality component models.

The forces plotted as a function of cumulative deformation in Figure 2b also illustrate the similarity of force-based and energy-based methods. Energy-based calibration (e.g., Chisari et al.[29]) focuses on the difference in the area of hysteresis loops (i.e., the area under the curves in Figure 2b). If a quadratic error function is used, the energy-based calibration error is calculated as follows:

$$\varepsilon_{\text{CAL,E}} = \int_d \left(F_s(d) - F_r(d)\right)^2 \mathrm{d}d \tag{2}$$

where $F_s(d)$ and $F_r(d)$ describe the simulated and reference response as a function of cumulative deformation. The calibration error in the force-based method can be considered a numerical approximation of the integral in Equation 2 that is calculated

using a Riemann sum. Given a sufficiently large number of equally spaced data points over the whole load history, the energy-based and force-based methods lead to similar results. Hence, the observations presented about the force-based method are also applicable to an energy-based method.

3.2 | Stiffness-hardening-based method

This calibration method aims to enhance calibration by focusing on features relevant to dynamic structural response. We identified three features of BRBF and illustrated their quantification in Figure 3:

- The first feature is *lateral stiffness* because it governs the seismic response of a frame structure. Lateral stiffness of a BRBF is primarily defined by the stiffness of its diagonal BRBs. The initial stiffness of those BRBs is usually captured with sufficient accuracy. The difficultly lies in modeling the inelastic stiffness characterized by strain hardening. The first feature focuses on the accuracy of the component model in this area. The development of BRB stiffness over a test can be investigated by estimating the gradient of the force response function at each data point. Constraining the range of stiffness (K) values of interest to $|K| < K_0/10$, where K_0 is the initial BRB stiffness, allows engineers to focus only on the inelastic BRB stiffness (see the stiffness range displayed in Figure 3b).

- The second feature is *cyclic hardening* (i.e., the gradual increase in load bearing capacity over consecutive load cycles) because it heavily influences the simulated response and potential failure of the non-dissipative components in a BRBF[30]. Cyclic hardening of a BRBF typically stems from the isotropic hardening of the steel core of BRBs. This isotropic hardening in test data can be investigated by focusing on the axial forces developed within the inelastic-response domains identified previously (i.e., the parts of the response history where $|K| < K_0/10$ in Figure 3).

- The third feature is *non-symmetric behavior* because the strain- and cyclic-hardening characteristics of a BRB are not identical under tension and compression and this makes component-model development difficult. Figure 2a illustrates the problem: given a component model limited to symmetric response, it is impossible to find a set of parameters that provides a good fit for BRB behavior under both tension and compression. However, consideration of the structural topology can lead to an efficient solution (see the note about the corresponding assumptions below). Braces in a BRBF are often arranged in a symmetric layout. During horizontal loading, half of the braces in such frames are under tension, and the other half are under compression. For every BRB there is a complementing one in the same story that experiences practically identical deformation history, but in the opposite direction. The behavior of such a BRBF does not depend on the load direction; it is symmetric at the structural level. It should be possible to capture that structural behavior with a symmetric component model as long as the calibration focuses on the response of a pair of BRBs that are loaded identically, but in opposite directions.

Note: The argument presented for using a BRB model with symmetric behavior assumes that the response of each BRBF story is governed only by its BRBs. This requires at least the following three assumptions to hold: i) the connections that link the BRB to the beam-column joint remain elastic; ii) the beams and columns connected to BRB elements remain elastic; and iii) the localized effects due to force imbalance between braces in tension and in compression are negligible. These are reasonable assumptions under small deformations, but they will not hold near collapse. We use the proposed model here as a simplified approach to BRB modeling to allow us to investigate calibration relevance. Before trying to estimate the real response of a BRBF with such a simple model, we recommend reviewing the assumptions listed above.

Rather than comparing reference and simulation results at each data point, calibration error in this method is based on the difference between average characteristics over the load history (see the dashed lines in Figure 3). Calibration error is assumed proportional to the error in the average inelastic tangent stiffness ($\overline{K}$) and average inelastic axial force ($\overline{F}$) of the BRB. The average characteristics are calculated under tension and compression independently (i.e, $\overline{K}^+$, $\overline{K}^-$, $\overline{F}^+$, $\overline{F}^-$) and summed up to get the characteristics corresponding to a pair of BRBs. The $^+$ and $^-$ superscripts identify characteristics corresponding to tension and compression, respectively. This approach recognizes that a pair of BRBs subjected to opposing load histories will exhibit a symmetric response that can be approximated by a symmetric component model.

The calibration error has two components in this method: error in stiffness ($\varepsilon_{\text{CAL,S}}$) and error in hardening ($\varepsilon_{\text{CAL,H}}$). Each error component is defined as the absolute log-ratio of simulated and reference characteristics:

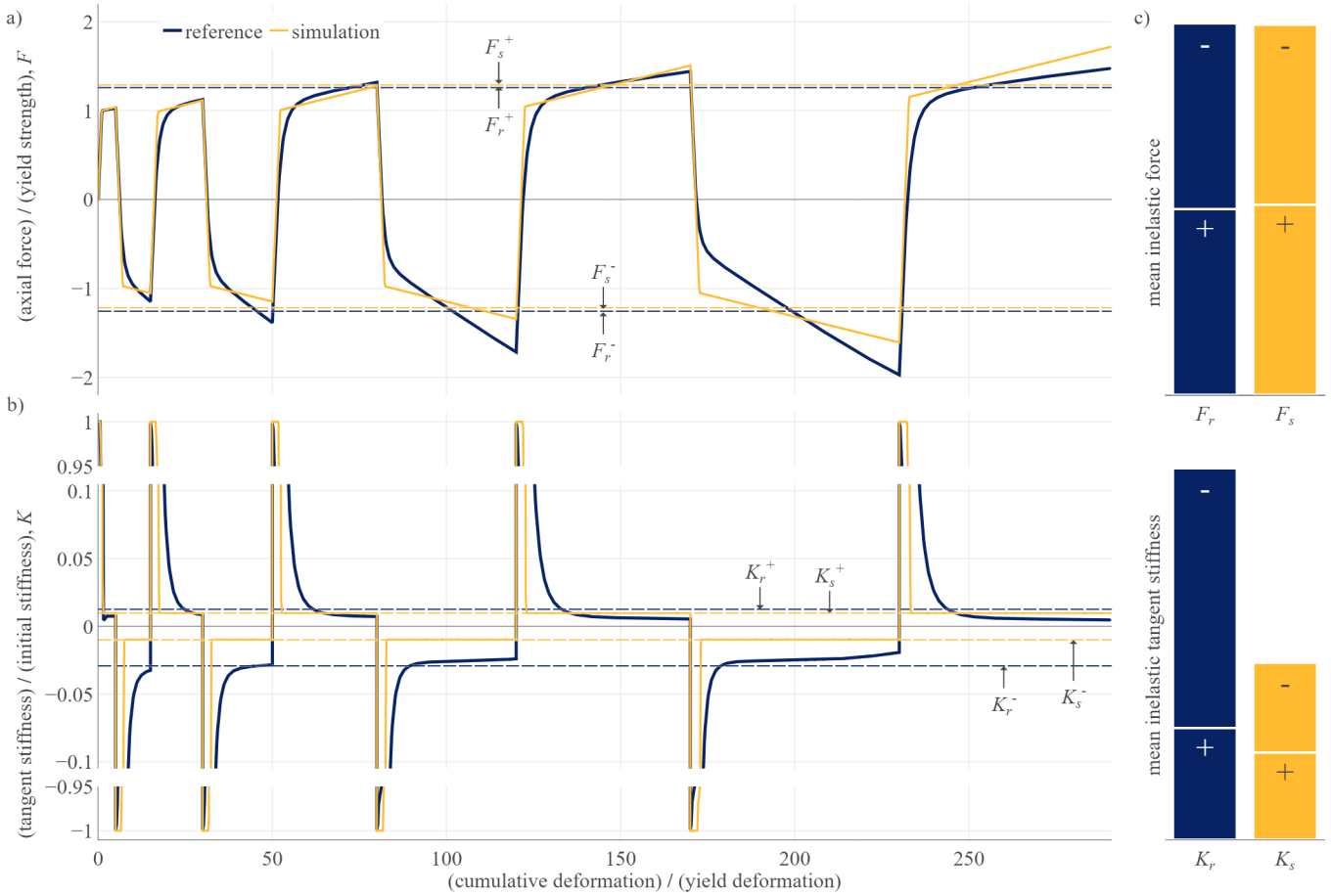

FIGURE 3 Calculation of the stiffness-hardening-based calibration error: a) force-cumulative deformation, and b) tangent stiffness-cumulative deformation responses; c) $\varepsilon_{\text{CAL,SH}}$ is based on the values of mean inelastic force and mean inelastic tangent stiffness for the reference and simulation responses.

$$\varepsilon_{\text{CAL,S}} = \left| \log \frac{\overline{K}_s^+ + \overline{K}_s^-}{\overline{K}_r^+ + \overline{K}_r^-} \right| \tag{3}$$

$$\varepsilon_{\text{CAL,H}} = \left| \log \frac{\overline{F}_s^+ + \overline{F}_s^-}{\overline{F}_r^+ + \overline{F}_r^-} \right| \tag{4}$$

The r and s subscripts correspond to reference and simulation characteristics, respectively. For example, $\overline{K}_s^+$ is the average simulated inelastic tangent stiffness under tension. The absolute value and logarithm functions are used to arrive at zero-based, non-negative error measures. The calibration error is the weighted sum of the two error components. The higher importance of inelastic stiffness is recognized by applying a weight of 2 to $\varepsilon_{\text{CAL,S}}$:

$$\varepsilon_{\text{CAL,SH}} = 2\varepsilon_{\text{CAL,S}} + \varepsilon_{\text{CAL,H}} \tag{5}$$

Figure 3b displays the average characteristics, the error components, and their contribution to the calibration error in the presented calibration example. The comparisons highlight that the simulated response provides an acceptable estimate of cyclic hardening ($\varepsilon_{\text{CAL,H}}$ is small because $\overline{F}_s^+ + \overline{F}_s^-$ is close to $\overline{F}_r^+ + \overline{F}_r^-$), but it underestimates the stiffness response of the pair of BRBs due to a severe underestimation of inelastic stiffness under compression ($\varepsilon_{\text{CAL,S}}$ is large because $\overline{K}_s^-$ is significantly higher than $\overline{K}_r^-$, while the average stiffnesses under tension are similar).

4 | FRAMEWORK OF VIRTUAL EXPERIMENTS

4.1 | Overview

The proposed framework of virtual experiments was designed to represent two important features of the mathematical problem of multi-level model calibration:

1. *Imperfection of the structural model*: The difference between reality and a structural model is captured by performing the virtual experiments on a high-fidelity (*reference*) and on a simplified (*simulation*) structural model. The reference model has several features that cannot be represented in the simulation model. Hence, the simulation model will be imperfect even when it is used with the optimal parameters.

2. *Imperfection of the calibration method*: The difference between dynamic and quasi-static environments (Figure 1) is captured directly by performing virtual experiments in each environment. Information about dynamic structural response is only used for evaluation of the calibration methods; it is not available for calibration purposes. Hence, the calibration methods will have imperfect information about the dynamic behavior of the simulation model.

A traditional sequence of steps to investigate the efficiency of calibration methods is as follows. After the identification of the reference structure and the primary component, the component models are calibrated using results of quasi-static component tests. Then, the simulation model is assembled from the calibrated component models. Finally, the accuracy of simulated dynamic structural response is evaluated by comparing the response of the reference model to the response of the simulation model. The main advantage of the proposed framework is that the dynamic response of the reference structure to any arbitrary dynamic excitation is available. This contrasts with the few reference results available from real, full-scale experiments.

Instead of the above traditional sequence, here we recommend performing the tasks following the order in Figure 4:

I Define the high-fidelity reference structural model that represents real behavior and identify its primary component(s).

II Simulation models of the structure are based on the reference structural model, but the primary components are replaced with simplified component models. Generate a set of simplified component models that cover the interesting part of the component-model parameter space.

III Perform virtual, full-scale, dynamic tests on the reference model and each simulation model. Evaluate the error in the dynamic response for every simulation model.

IV Perform a virtual quasi-static component test on the reference component according to a prescribed load protocol.

V Determine the calibration error for every simplified component model using each calibration method of interest.

VI Compare calibration error ($\varepsilon_{\text{CAL,F}}$ and $\varepsilon_{\text{CAL,SH}}$ in this paper) to the error in dynamic response simulation (ε_{DYN}, introduced later) for every simulation model to evaluate the efficiency of various calibration methods.

The general methodology above is applicable to a wide range of structural systems and calibration methods. The following details demonstrate its application to investigate BRBF modeling and calibration.

4.2 | Reference model

The virtual, full-scale, dynamic tests are performed on a reference BRBF model in the OpenSEES finite element environment [31]. The reference, state-of-the-art, BRBF model was developed to aid BRBF design procedure standardization efforts in Europe [32]. Figure 5 shows a BRBF archetype and how such a design is represented in OpenSEES. Details of the reference BRBF model are described in Zsarnóczay and Vigh [31].

BRB-element modeling deserves special attention because the majority of BRBF response is explained by the behavior of its BRBs. The reference BRBF uses a complex BRB component model that provides a highly accurate representation of the nonlinear cyclic-hardening behavior of BRBs. Component tests have shown slight influence of BRB capacity (i.e., cross-section size of the BRB steel core) on BRB hardening characteristics. Such influence is not taken into consideration in this research for the sake of simplicity. Hence, all BRB elements are modeled using the Steel4 material in OpenSEES with the *reference BRB*

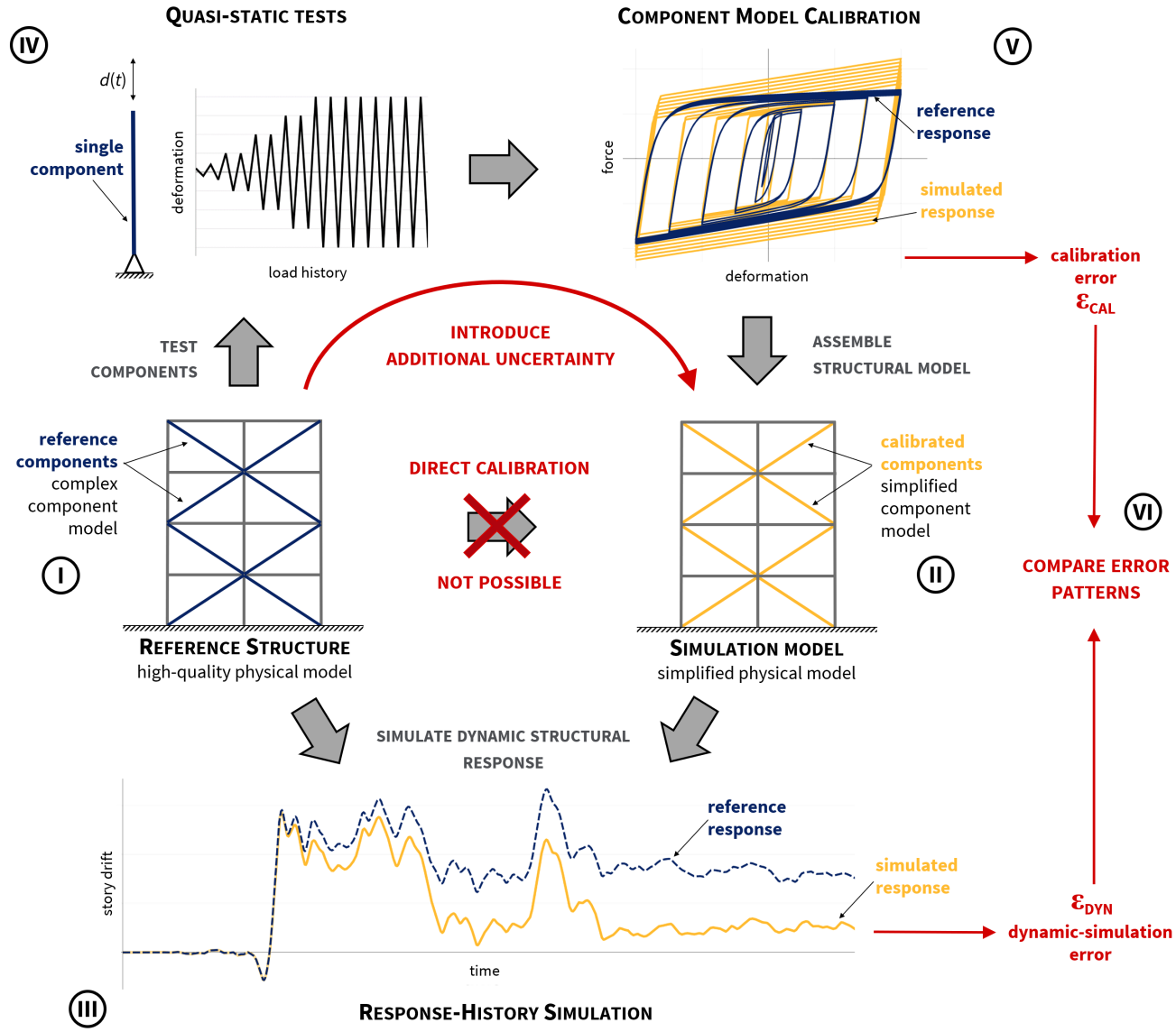

FIGURE 4 The proposed framework of virtual experiments to evaluate the efficiency of calibration methods

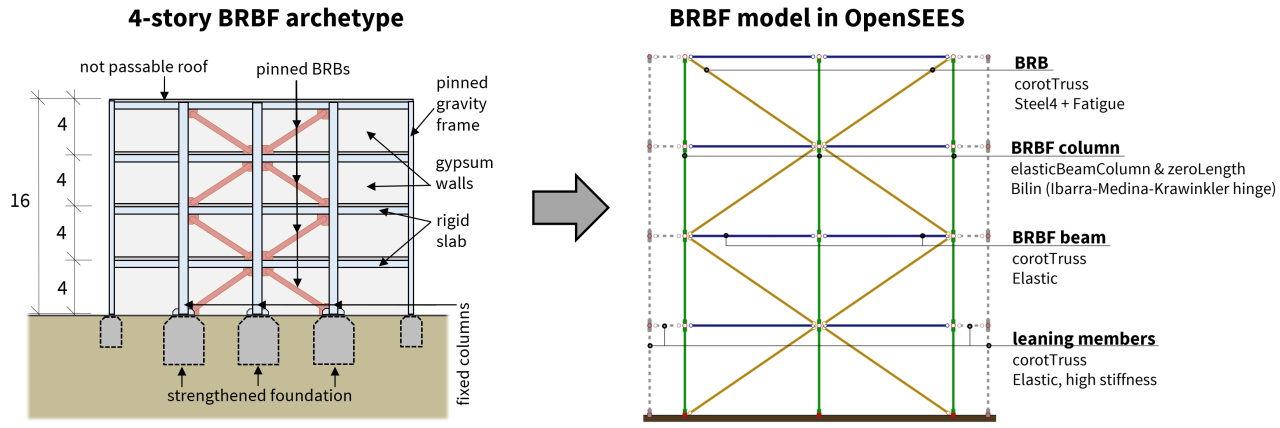

FIGURE 5 The reference Buckling Restrained Braced Frame archetype and its representation in OpenSEES.

TABLE 1 Parameters of the Steel4 materials used in the reference and the simulation BRB component models.

	reference BRB		simulation BRB
	tension	compression	symmetric
E_0	$E_s f_{SM}$		$E_s f_{SM}$
f_y	$\gamma_{m,ov} f_{y,k}$		$\gamma_{m,ov} f_{y,k}$
b_k	0.5 %	2.5 %	variable
R_0	25.0		50.0
r_1	0.91	0.89	0.92
r_2	0.10	0.02	0.01
b_i	0.25 %	0.6 %	variable
b_l	0.01 %	0.03 %	b_i
ρ_i	0.3		0.3
R_i	3.0		3.0
l_{yp}	1.0		0.0
f_u	1.65 f_y	2.40 f_y	N/A
R_u	2.0		N/A

parameters in Table 1. Figure 6 illustrates how these parameters control the simulated cyclic response of the Steel4 material. Zsarnóczay[33] provides more details about the phenomenological constitutive model used in Steel4.

The BRB component model requires basic inputs that are typically given by the BRB manufacturer. The following basic inputs are used to describe the material properties of the steel core: $f_{y,k} = 235$ MPa; $\gamma_{m,ov} = 1.13$; $E_s = 210$ GPa. The so-called stiffness modification factor (f_{SM}) is geometry-dependent and it is calculated individually for each brace in the BRBF using the expressions described in Vigh et al.[32]. Its value is available for the reference and the simulation components as well.

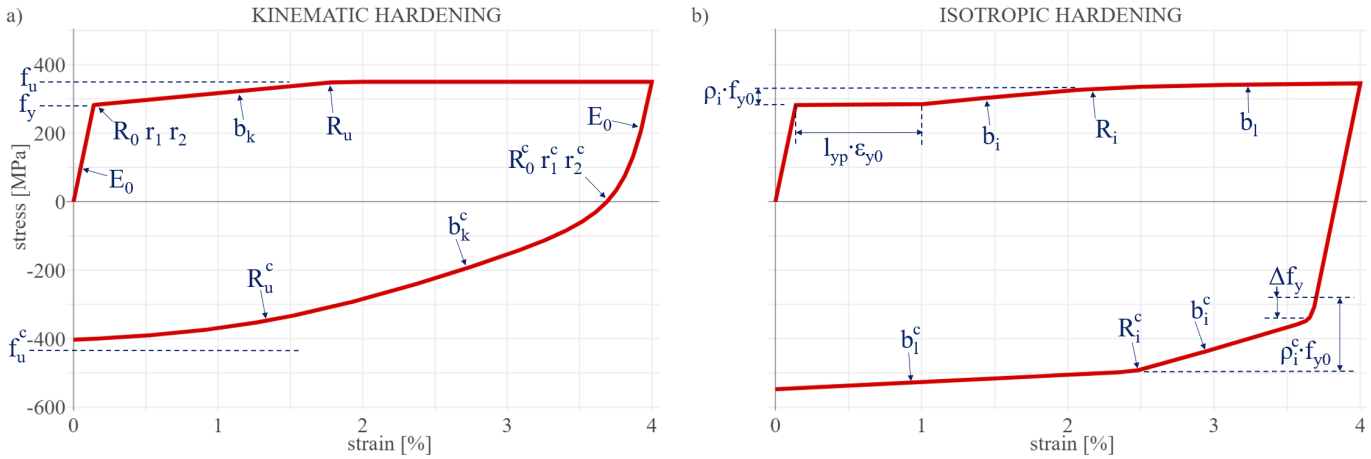

FIGURE 6 Examples of non-symmetric cyclic responses simulated by the Steel4 material in OpenSEES. The responses illustrate how each parameter controls the kinematic (a) or isotropic (b) hardening of the constitutive model. Parameters with no superscript correspond to tension; those with a "c" superscript correspond to compression. Δf_y in b) shows the increase in the yielding point due to isotropic hardening in the first half-cycle.

4.3 | Simulation models

The only difference between the simulation models and the reference model is the approach to BRB-element modeling. Simulation models describe BRB response by a symmetric, bilinear-hardening behavior that uses a combination of kinematic and isotropic hardening. Assuming that the initial stiffness (E_0) and the yield strength (f_y) of the BRB can be identified with sufficient accuracy, calibration of a simplified component model needs to focus on the two remaining unknown parameters: b_k and

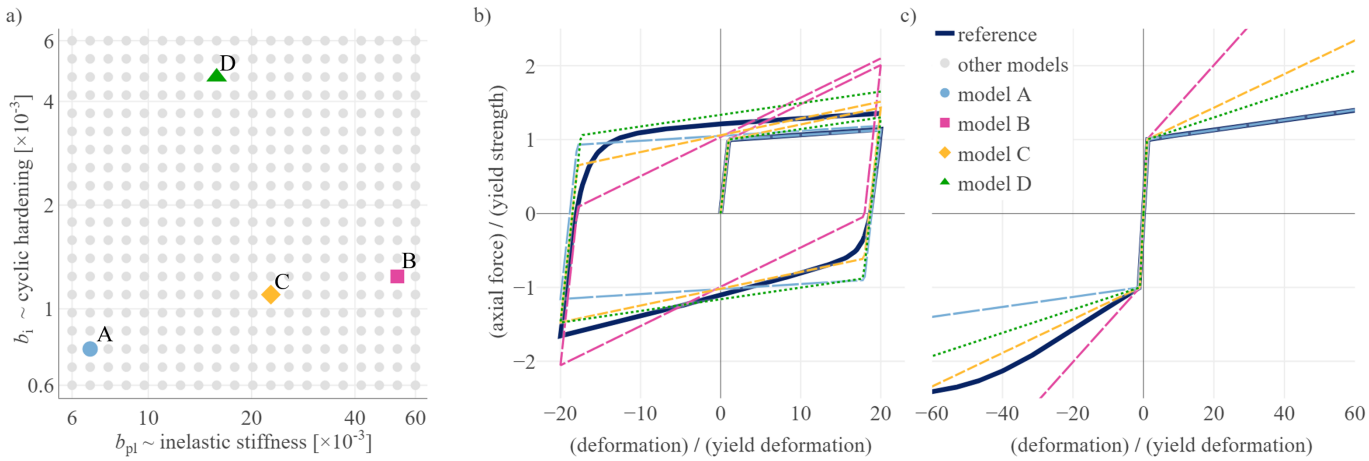

FIGURE 7 Illustration of the simplified component model candidates: a) 400 candidates displayed in the space of the component-model parameters; b) cyclic responses of four highlighted example models; c) monotonic responses of the same four example models.

b_i. Such an approach is frequently used for BRB modeling in the literature and in design practice; sometimes even without the consideration of isotropic hardening[34,35]. The *simulation BRB* parameters in Table 1 show how the simplified component model is represented using the Steel4 material in OpenSEES.

Although the simplified component model can simulate various cyclic responses, calibrating its parameters to capture the response of a BRB is not a trivial task. The four example models in Figure 7 illustrate that different features of the reference component response are captured by using different (b_i, b_k) parameters. Calibration is about choosing which features of the BRB response shall be prioritized and searching for the most reliable simplified component model that reproduces those features with the smallest error.

Figure 7a shows the two-dimensional component-model parameter space for the simplified component model. The space is spanned by the (b_{pl}, b_i) parameters. The first parameter, $b_{pl} = b_k + b_i$, is proportional to the slope of the inelastic asymptote of the bilinear response (see Figure 7b and c) and is often referred to as inelastic stiffness, or strain hardening ratio in the literature[34]. The second parameter, b_i, is proportional to the magnitude of strength-increase in consecutive load cycles, hence it is referred to as cyclic hardening.

We defined a set of 400 simplified component models in this space that are considered candidates for the simulation of the dynamic response of the reference BRBF. Each model is represented by a gray marker in Figure 7a. Four models are highlighted to illustrate the range of models considered and to serve as examples in subsequent figures of the paper:

- Model *A* has low inelastic stiffness and negligible cyclic hardening. Its inelastic stiffness is identical to that of the reference BRB under tension.
- Model *B* has high inelastic stiffness and low cyclic hardening. Its inelastic stiffness exceeds that of the reference BRB under compression.
- Model *C* has an intermediate level of inelastic stiffness and low cyclic hardening. Its inelastic stiffness is between that of the reference BRB under tension and compression. (We show later that this model can simulate the dynamic response of the reference BRBF with the smallest error.)
- Model *D* has an intermediate level of inelastic stiffness and high cyclic hardening. Although both are intermediate, the inelastic stiffness of model *D* is significantly less than that of model *C* (note the logarithmic scale in Figure 7a). The lack of inelastic hardening is compensated by the considerable strength increase in consecutive load cycles.

4.4 | Dynamic response

Dynamic structural response is characterized by the peak interstory drift (i.e., the temporal maximum of the governing interstory drift ratio among all stories of the structure) in this study. The uncertainty of the seismic hazard is modeled by running analyses

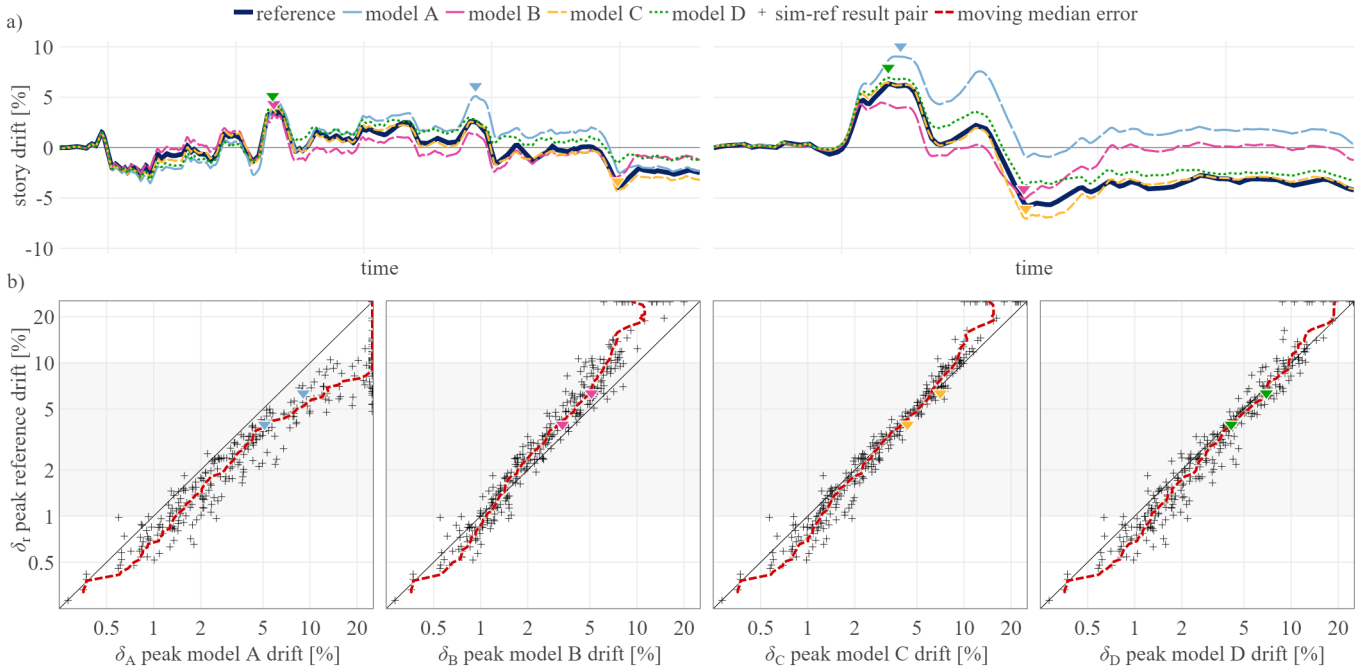

FIGURE 8 Evaluation of error in dynamic response simulation through the example of four simulation models: a) two response history samples with peak interstory drifts highlighted for each simulation model; b) reference-simulation peak interstory drift pairs from 300 dynamic response simulations for each simulation model. The moving median error curves illustrate the dependence of model error on reference drift magnitude.

with a large number of ground motion records and considering each result as a sample of the random structural response. We use 100 ground motion records: the Far Field and the Near Field sets defined in FEMA P-695[3].

The 100 ground motions are each scaled by factors of 0.35, 0.95, and 1.80. The scale factors were chosen to provide a large number of uniformly distributed peak interstory drift (δ) samples in the 1%-10% drift range. Out of the 300 dynamic response history analyses with the reference BRBF model, 203 led to peak interstory drifts between 1% and 10% (δ_r ordinates in the scatter plots in Figure 8b). These analyses were performed with every simulation model as well. The δ_s ($s \in [A, B, C, D]$) abscissas in the scatter plots in Figure 8b correspond to the results with the previously introduced example models.

The difference between δ_r and δ_s is used to quantify the error in dynamic response simulation for each simulation model. Perfect results are located on the black diagonals in Figure 8b. The bias in dynamic simulation is described by calculating the median δ_s in a moving δ_r window. The resulting moving-median δ_s curves (red dashed lines in Figure 8b) reveal that simulation models with approximately zero expected bias in the 1%-10% drift range (e.g., models B-D) show a general tendency to overestimate small drifts and underestimate large ones. This behavior stems from the imperfection of the simplified component model: an overall appropriate bilinear approximation of the nonlinear behavior will underestimate stiffness at small strains and overestimate it at large strains (compare, for example, the monotonic response of model *C* to the reference response in Figure 7c. Partitioning the drift domain of interest into a set of sufficiently small sub-domains, and using an appropriate (i.e., approximately unbiased) simulation model in each sub-domain can eliminate drift-dependent bias and significantly reduce the uncertainty due to model error. This phenomenon is especially important for loss-assessment studies that use simulated drifts as proxies for structural damage, but its detailed investigation is out of the scope of this paper.

We define the error in dynamic response simulation as the root-mean-squared log-relative difference between simulated and reference peak interstory drifts:

$$\epsilon_{\text{DYN}} = \sqrt{\frac{1}{N}\sum_{i=1}^{N}\left(\log \delta_{s,i} - \log \delta_{r,i}\right)^2} = \sqrt{\frac{1}{N}\sum_{i=1}^{N}\left(\log \frac{\delta_{s,i}}{\delta_{r,i}}\right)^2} \tag{6}$$

FIGURE 9 Load protocol applied in virtual quasi-static tests

where N is the number of available dynamic response samples. This error measure punishes simulation models that exhibit the aforementioned drift-dependent bias without the need to quantify the relationship between δ_r and the bias. It is reasonable to assume that the expected bias of the optimal simulation model is zero (see, for example, the performance of model C in the 2%-5% drift range in Figure 8b). For such a model $\varepsilon_{\mathrm{DYN}}$ is an estimate of the logarithmic standard deviation of $\delta_s|\delta_r$. This quantity is often prescribed in modern PSPA guidelines as added variance to consider model uncertainty (β_{m})[14]. Consequently, minimizing $\varepsilon_{\mathrm{DYN}}$ can be interpreted as looking for the simulation model that adds the least amount of uncertainty to dynamic response simulation results.

4.5 | Virtual quasi-static experiments

The simplified component model calibration is based on force-deformation response of the reference BRB model in virtual quasi-static uniaxial component tests. The virtual tests are deformation-controlled nonlinear static analyses performed in OpenSEES. Following the recommendations of various standards[36,37] and common research practice[38,39], the applied load protocol comprises a series of groups of load cycles with monotonically increasing deformation amplitude (Figure 9).

The virtual tests return the true force-deformation response of the reference component - measurement error and other test-related uncertainties are not simulated in this research. Using the virtual test data and the calibration methods introduced earlier, we evaluated $\varepsilon_{\mathrm{CAL,F}}$ and $\varepsilon_{\mathrm{CAL,SH}}$ for each simplified component model from Figure 7a.

5 | RESULTS

5.1 | Error in dynamic response simulation

The error in dynamic response simulation is evaluated for every simulation model and visualized in the $(b_{\mathrm{pl}}, b_{\mathrm{i}})$ space that was introduced earlier (see Figure 7a). The $\varepsilon_{\mathrm{DYN}}$ data in Figure 10a provide perfect information about the performance of the simulation models. If such data were available, they would enable direct calibration of the simulation model and the parameters that minimize $\varepsilon_{\mathrm{DYN}}$ could be identified.

Model uncertainty would be present in dynamic response simulations even in such an ideal scenario. The error in dynamic response of the optimal simulation model (highlighted by the yellow diamond marker of model C) is 0.15. The corresponding model uncertainty can be considered by adding a random error with log-standard deviation of 0.15 to the drifts from dynamic response simulation.

If a $\beta_{\mathrm{m}} = 0.15$ model uncertainty is combined with a typical[14] record-to-record uncertainty of $\beta_{\mathrm{RTR}} = 0.4$, the majority of the total uncertainty will be due to β_{RTR}. This suggests that the simulation model can be used to estimate the response of the reference model with sufficient accuracy if it is used with the optimal parameters. This observation is also supported by the good agreement between the reference and simulated drifts in the scatter plot that corresponds to model C in Figure 8b. Furthermore, the two example drift histories in Figure 8a show that not only the peak interstory drift, but the entire drift response of model C is in good agreement with the response of the reference model.

There is one important caveat: even a small deviation from the optimal parameters can increase the error in the simulation and the corresponding model uncertainty significantly. Figure 10a shows that changing the b_{pl} parameter of the optimal model C by

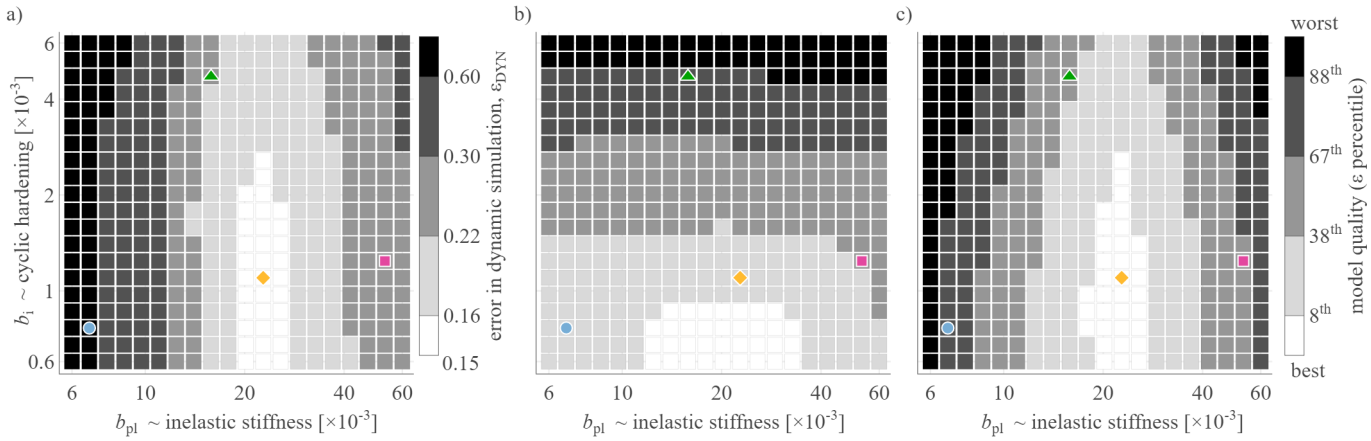

FIGURE 10 Error in a) dynamic response simulation; b) force-based calibration; c) and stiffness-hardening-based calibration as a function of the component-model parameters. Models *A*, *B*, *C*, and *D* from Figure 7 are highlighted using the same symbols.

less than 20% results in simulations with 150%-200% of the minimum uncertainty. Such high values of β_m become important contributors to the total uncertainty in the dynamic response simulation. Extreme cases towards the edge of the parameter space go well-beyond those levels. These results emphasize that the utility of a particular structural model depends not only on its performance given an optimal set of parameters, but also on the likelihood that we will be able to identify those parameters.

5.2 | Error in component calibration

The results in Figure 10a required 203 (virtual) full-scale, dynamic tests on the reference BRBF. Because performing such a large number of physical, full-scale tests is not feasible in reality, ε_{DYN} is inferred from calibration error (Fig 4). Figure 10b and c display the force-based ($\varepsilon_{CAL,F}$) and stiffness-hardening-based ($\varepsilon_{CAL,SH}$) calibration errors, respectively, for the 400 simplified models in the (b_{pl}, b_i) parameter space.

Rather than looking at the calibration error value, the simulation models are ranked by their calibration error and classified into five groups. The brightness of each cell in the figure identifies the group of the corresponding model. The groups represent ranges of percentiles identical to those in Figure 10a. The best simulation models, for example, have $\varepsilon_{DYN} < 0.16$. These are the top 8% of all simulation models and are identified by the white cells in Figure 10a. Cells with the same color in Figure 10b and c represent the top 8% of simulation models based on their $\varepsilon_{CAL,F}$ and $\varepsilon_{CAL,SH}$ calibration error measure, respectively.

The cell color pattern of force-based calibration error in Figure 10b is different from the dynamic simulation error pattern in Figure 10a. This illustrates that simulation models have different relative value in force-based calibration and dynamic response simulation. Each highlighted marker in the figure corresponds to one of the simulation model examples that were introduced earlier. A comparison of model *A* (blue circle) and model *C* (yellow diamond) illustrates the disagreement between ε_{DYN} and $\varepsilon_{CAL,F}$ very well: on the one hand, according to force-based calibration, both models are better than average, but not in the best group; on the other hand, the large error in dynamic simulation puts model *A* in the worst 12% of models, while model *C* provides the lowest dynamic response simulation errors among all 400 simulation models.

The calibration error is approximately uniform along the horizontal axis in Figure 10b, which suggests that force-based calibration is insensitive to inelastic stiffness of the simplified component model and it primarily focuses on cyclic hardening characteristics. The large cyclic hardening of model *D* (green triangle) leads to a large $\varepsilon_{CAL,F}$ calibration error. Force-based calibration suggests that model *D* is the worst-performing simulation model among the four examples, while dynamic simulation results show that its performance is second only to model *C*.

The cell color pattern of stiffness-hardening-based calibration error in Figure 10c is in good agreement with the dynamic simulation error pattern in Figure 10a. The calibration error captures the importance of both inelastic stiffness and cyclic hardening. The ranking of example models is identical in Figure 10a and c. This suggests that the stiffness-hardening-based calibration method is more relevant to dynamic structural response simulation than the force-based method; i.e., using $\varepsilon_{CAL,SH}$ we can infer ε_{DYN} and select the simplified component models that provide the smallest errors in dynamic response simulations.

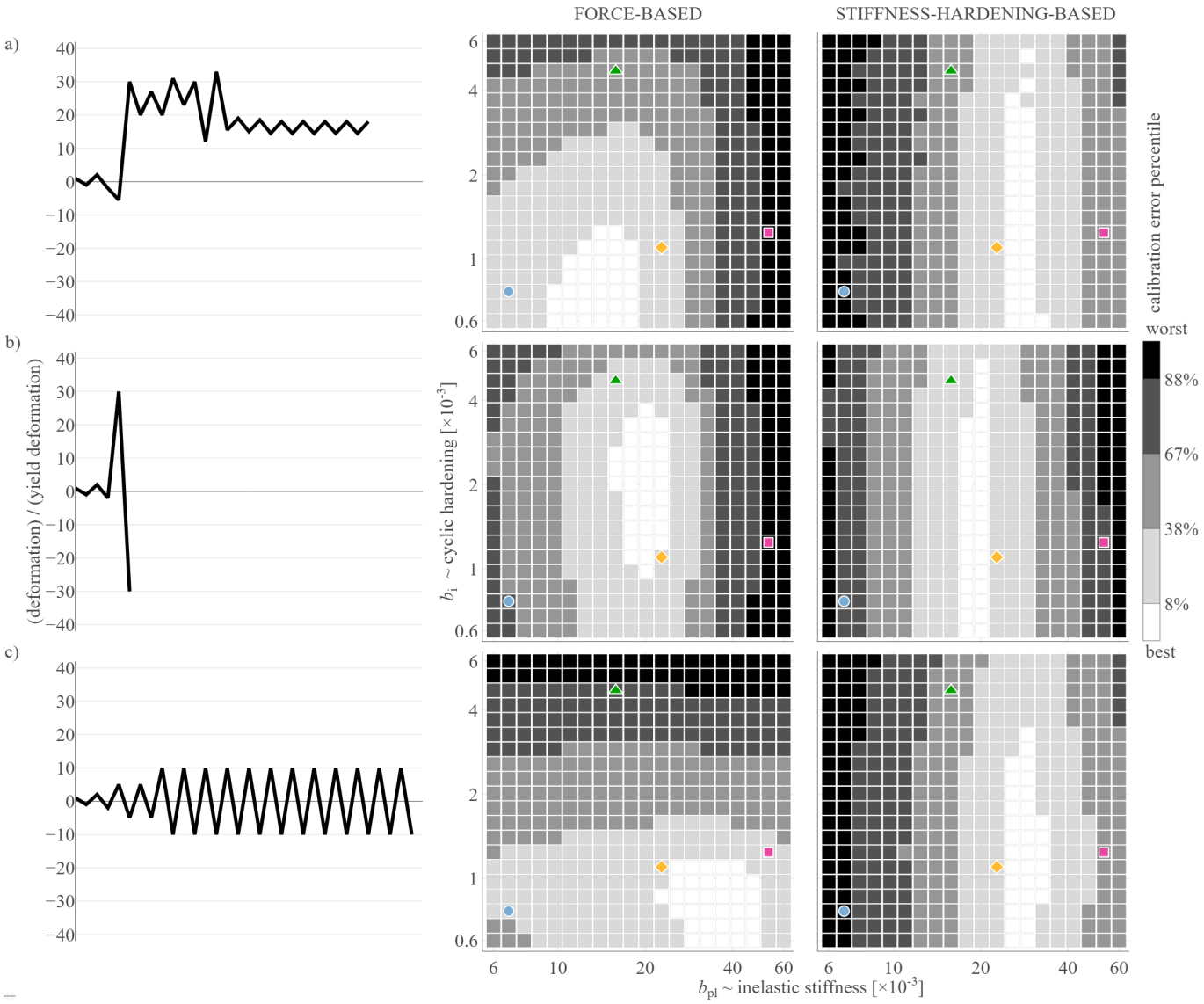

FIGURE 11 Force-based and stiffness-hardening-based calibration error is shown for a) a realistic; b) a pulse-like; c) and a fatigue-focused load history. Models *A*, *B*, *C*, and *D* from Figure 7 are highlighted using the same symbols.

6 | DISCUSSION

6.1 | Influence of load protocols

The applied load protocol in Figure 9 describes a different cyclic response than the one experienced during seismic excitation. Recognizing that the applied load protocol influences calibration relevance (i.e., the ability to infer dynamic response simulation error from calibration error), several researchers advocate the use of more realistic protocols which represent the response of the primary component during an earthquake[40,41]. We argue that the transformation from dynamic to quasi-static loading (Figure 1) obscures a considerable portion of the information about structural behavior, and using a more realistic load protocol will not necessarily provide more or higher quality information. Figure 11 supports this argument by showing calibration error patterns conditioned on three different quasi-static load protocols.

The difference in calibration error patterns in Figure 11 and Figure 10 is explained in part by the nonlinear behavior of the reference component. The reference inelastic stiffness gradually decreases as the strain amplitude increases, and cyclic hardening saturates after a certain amount of energy has been dissipated by the component. The size and the number of load cycles in an experimental load protocol heavily influences the amount of information available about these phenomena.

Part a of Figure 11 displays a protocol based on the dynamic response of the reference component in Figure 1. This realistic protocol focuses on tension and provides hardly any information about compression. There are only a few half-cycles with high or moderate deformation amplitudes, which makes it difficult to estimate the hardening characteristics of the element. The short compression half-cycles emphasize the initial part of the nonlinear hardening behavior. This initial part has significantly larger tangent stiffness than compression response at larger strains. The issues above lead to an overestimation of the optimal inelastic stiffness by $\varepsilon_{\mathrm{CAL,SH}}$. The force-based method does not differentiate between load directions and weighs all data points equally. Consequently, its calibration risk is governed by the small stiffness of the large tension half-cycle. Cyclic hardening plays a smaller role when this load protocol is used because there is only little information available about it. This explains the increased sensitivity of $\varepsilon_{\mathrm{CAL,F}}$ to b_{pl}.

Force-based calibration sensitivity to inelastic stiffness is increased even further by the pulse-like load protocol in Figure 11b that provides practically no information about cyclic hardening. The longer compression half-cycle emphasizes inelastic stiffness under compression and the resulting error pattern is the best among the tested cases for force-based calibration. The alternative $\varepsilon_{\mathrm{CAL,SH}}$ error pattern provides superior results that are very similar to those in Figure 10 and is able to identify the high-quality models.

Finally, the third load protocol in part c illustrates an experiment with only moderate deformation amplitudes, but a large number of load cycles. Such load protocols are common when specimens are tested for their low cycle fatigue performance[42]. It has been recognized in the literature that these protocols impose significantly higher cumulative deformation demand on the components than even a collapse-inducing ground motion would[43]. Consequently, following the second part of the experienced cyclic hardening development is not relevant to dynamic response simulation. Any calibration method that takes the complete hardening history into account and focuses on cyclic hardening will be misled by this data. Furthermore, the lack of information about inelastic stiffness makes it difficult to evaluate b_{pl} with sufficient accuracy in this scenario. Similarly to part a), the stiffness-hardening method is controlled by the large tangent stiffness of the reference model under compression and slightly overestimates the optimal inelastic stiffness. The focus of the force-based method is cyclic hardening, with inelastic stiffness hardly playing any role in the calibration.

A comparison of the two calibration methods across the three parts of Figure 11 reveals that $\varepsilon_{\mathrm{CAL,SH}}$ is superior to $\varepsilon_{\mathrm{CAL,F}}$ in all cases because it reliably estimates the dynamic response error pattern displayed in Figure 10a. The force-based calibration is more sensitive to changes in the load protocol because it uses the force-deformation data directly. The stiffness-hardening-based calibration exhibits more consistent performance because information about the features it uses is available from most experiments.

These results demonstrate that load protocols should be evaluated based on the information they provide about the important features of the component. In the particular example of $\varepsilon_{\mathrm{CAL,SH}}$ presented in this paper, the important features are inelastic stiffness in a sufficiently large strain range and cyclic hardening corresponding to a realistic amount of dissipated energy. A load protocol that emphasizes these features does not need to mimic dynamic response of the primary component. This observation gives more flexibility for load-protocol design from a model calibration perspective and allows the protocol-designer to accommodate other experimental objectives as well.

6.2 | Higher-fidelity component models

Choosing a relevant calibration method becomes important when the difference between the simulation and the reference response cannot be reduced to zero by using the optimal set of parameters. The component model with a bilinear cyclic response used in this research to represent the simplified BRB component model clearly presents such a case. Component models of higher fidelity can produce complex nonlinear responses that seem to be in considerably better agreement with the reference results. Visual inspection of force-deformation plots might suggest that the imperfections in such high-fidelity component models are negligible and, consequently, their calibration can be performed by any method, even by visual trial and error. The following example demonstrates how misleading such visual inspections can be and how much more engineers can learn by using a calibration method that focuses on important features of the dynamic component behavior.

Figure 12a and b show two different component models calibrated to the safe reference BRB response. The reference response is from a real laboratory test[44], and the component models take advantage of the complex material model that was used earlier in the paper to represent the real behavior (Table 1). The calibration methods presented earlier were used to prepare two component models:

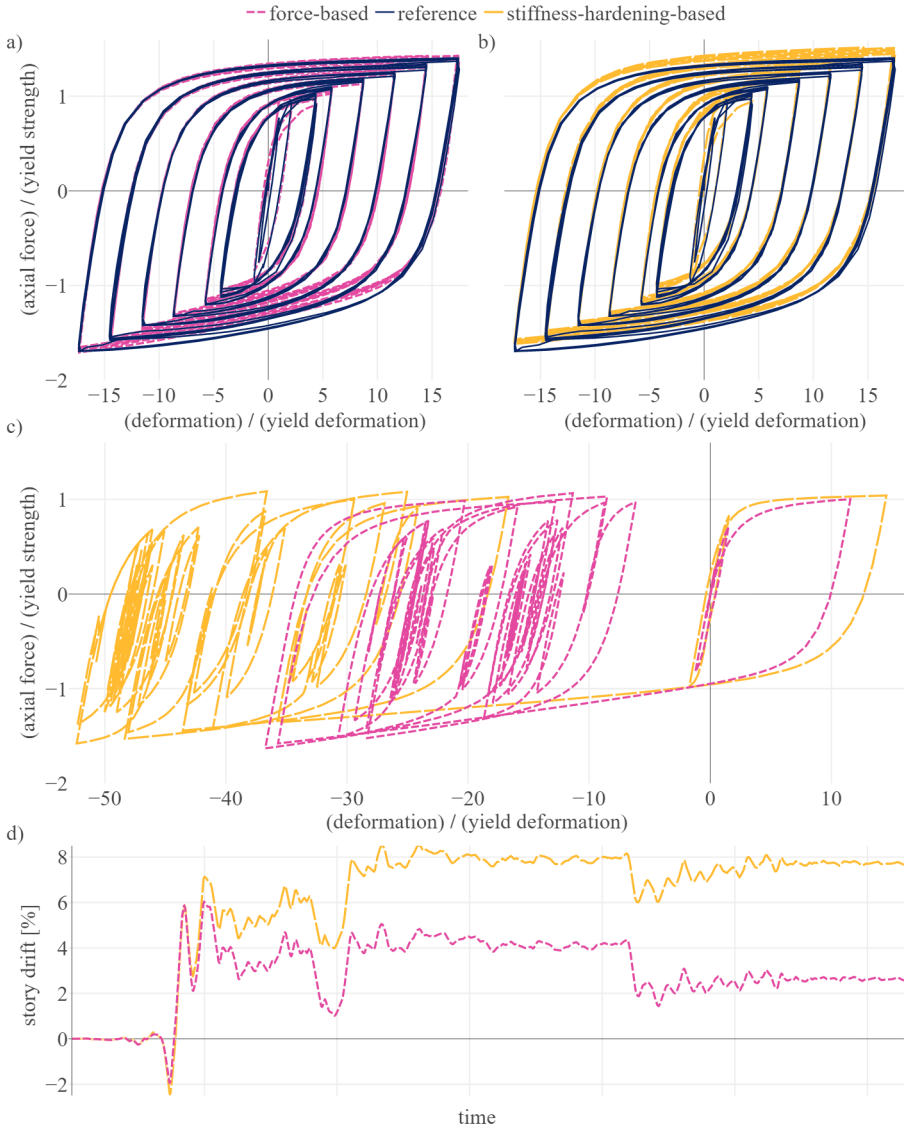

FIGURE 12 Comparison of the responses of two high fidelity models: cyclic response of the optimal component model in a) force-based and b) stiffness-hardening-based calibration; c) cyclic response of the two component models in a structure under earthquake loading; d) interstory drift response of the structure

1. The force-based model minimizes the $\varepsilon_{\text{CAL,F}}$ force-based calibration error (Figure 12a). In quasi-static tests the model simulates force and stiffness with minimal error under tension. Under compression, there is a slight error in force and a significant error in tangent stiffness.

2. The stiffness-hardening-based model minimizes the $\varepsilon_{\text{CAL,SH}}$ stiffness-hardening-based calibration error (Figure 12b). In quasi-static tests the model simulates tangent stiffness with minimal error in both load directions, but it overestimates force under tension and underestimates it under compression. However, when two BRBs are put in a chevron configuration, the two errors in forces cancel each other and the total lateral resistance of the pair of BRBs is accurately simulated.

The advantages of the stiffness-hardening-based model are not immediately apparent in Figure 12a and b. We expect that a calibration based on visual inspection would favor the force-based model because it provides a better match for the force-displacement response.

One might argue that the difference between the two models is not significant. Figure 12c shows the cyclic response of the first-floor BRB in the four-story building from Figure 5 simulated using the two component models above. Due to its larger stiffness

under compression, the force-based model predicts significantly smaller deformations. This behavior is apparent already after the first major excursion. The stiffness of the BRBs heavily influences the global structural response as well: the simulated peak interstory drift in Figure 12d is 42% larger with the second model and it occurs at a different time-step.

We cannot compare the dynamic results to reference data because the reference in this example is the real behavior and real, full-scale, dynamic tests of the BRBF are not available. Even without such a comparison, Figure 12 demonstrates the potential for significant differences in simulated dynamic response of models that look similar during component calibration. This reinforces the need for better calibration methods than visual trial and error and the widely used force-based calibration.

7 | CONCLUSIONS

This paper focuses on improving the calibration of structural component models to reduce the model uncertainty in dynamic response-history simulations. Calibration methods often use results from quasi-static experiments to identify the best models for dynamic simulations. Since the calibration and the simulation environments are different, if a calibration method wants to provide optimal parameters for simulation, it has to focus on features of the component response that are important from the perspective of global structural behavior. Relevance describes how efficiently a calibration method can focus on such important features.

We propose a methodology to investigate the influence of calibration relevance on the model error in dynamic simulations. Real experiments are replaced by virtual tests on high-fidelity reference models. Human-made simulation models are represented by simplified versions of the reference models. Virtual quasi-static component tests are used to estimate a calibration error for a large number of simulation-model candidates Virtual dynamic tests are used to estimate the error in dynamic response simulation. Calibration relevance is discussed by comparing the order of simulation model candidates when ranked by calibration error to their order when ranked by the error in dynamic response simulation. The ranking provided by a relevant calibration method is in good agreement with the ranking from dynamic response simulation.

We used a BRBF model as a vehicle to demonstrate how calibration-related decisions influence errors in dynamic response simulation. Conventional force-based and energy-based calibration did not perform well. They failed to distinguish the high-quality simulation models from the low-quality ones. An efficient calibration method can compensate for the sparsity of experimental data by using knowledge in the field of structural dynamics and by recognizing organizational features of the structural system. We proposed a stiffness-hardening-based calibration method that focuses on the inelastic stiffness and cyclic-hardening characteristics of the BRBs. This method successfully identified high-quality simulation models in every presented scenario and performed significantly better than the conventional methods.

The applied load protocol heavily influences the utility of quasi-static experimental data. Well-designed load protocols provide ample information to engineers about the important features of the structural component. The fact that they represent dynamic component response during an earthquake does not make realistic load protocols better than others. Load protocols shall only be evaluated after the researcher specifies the important features of the component and how they are going to measure calibration error.

The variance of error in dynamic simulations is so significant that a single, full-scale, dynamic test of a structure is unlikely to provide sufficient information to quantitatively evaluate simulation models or calibration methods. It seems more feasible to develop high-fidelity simulation models of the important structural systems that can simulate dynamic response with sufficient accuracy, and calibrate those models with the limited number of available dynamic full-scale, and quasi-static component test results. Engineers could use such models to perform a large number of virtual experiments, and use the concept of calibration relevance and the framework proposed here to identify important features of the structural system and improve calibration methods. An iterative approach could use the improved calibration methods to re-calibrate the high-fidelity model, update the results of virtual experiments and perform another step of improvement in the calibration methods. These steps could be repeated until the model parameters converged to a solution.

The application of these results is limited by the type of BRBF examined in the study. We expect qualitatively identical findings for other frames with braces characterized by a balanced inelastic response with cyclic hardening. Expanding the scope to more complex structural systems is non-trivial. Structures with cyclic strength and stiffness degradation, or others composed of multiple types of components with inelastic behavior are particularly interesting from a practical perspective. The methodology proposed here has the potential to facilitate and systematize the improvement of component calibration methods

with a larger scope that includes those complex structural systems.

8 | ACKNOWLEDGEMENTS

The Thomas Cholnoky Foundation supported this research through the Imre Korányi Civil Engineering Fellowship. We thank Thomas Cholnoky and his family for providing the financial support that made this research possible. We also thank two anonymous reviewers for their insightful comments.

References

1. American Society of Civil Engineers ASCE ., ed.*ASCE/SEI, 41-17, Seismic Evaluation and Retrofit of Existing Buildings*. Reston, Virginia: American Society of Civil Engineers . 2017.

2. Naeim F. Performance-Based Seismic Design of Tall Buildings—A USA Perspective. In: Kasimzade AA, Şafak E, Ventura CE, Naeim F, Mukai Y., eds. *Seismic Isolation, Structural Health Monitoring, and Performance Based Seismic Design in Earthquake Engineering*Cham: Springer International Publishing. 2019 (pp. 249–274).

3. ATC ATC., ed.*FEMA P695: Quantification of Building Seismic Performance Factors*. Federal Emergency Management Agency . 2009.

4. Ibarra L, Krawinkler H. Global Collapse of Frame Structures under Seismic Excitations. Blume Report 152, Blume Earthquake Engineering Center, Department of Civil and Environmental Engineering, Stanford University; 2005.

5. Kwon OS, Elnashai A. The effect of material and ground motion uncertainty on the seismic vulnerability curves of RC structure. *Engineering Structures* 2006; 28(2): 289–303. doi: 10.1016/j.engstruct.2005.07.010

6. Padgett JE, DesRoches R. Sensitivity of Seismic Response and Fragility to Parameter Uncertainty. *Journal of Structural Engineering* 2007; 133(12): 1710–1718. doi: 10.1061/(ASCE)0733-9445(2007)133:12(1710)

7. Dolsek M. Incremental dynamic analysis with consideration of modeling uncertainties. *Earthquake Engineering & Structural Dynamics* 2009; 38(6): 805–825. doi: 10.1002/eqe.869

8. Liel AB, Haselton CB, Deierlein GG, Baker JW. Incorporating modeling uncertainties in the assessment of seismic collapse risk of buildings. *Structural Safety* 2009; 31(2): 197–211. doi: 10.1016/j.strusafe.2008.06.002

9. Kazantzi A, Vamvatsikos D, Lignos D. Seismic performance of a steel moment-resisting frame subject to strength and ductility uncertainty. *Engineering Structures* 2014; 78: 69–77. doi: 10.1016/j.engstruct.2014.06.044

10. Gokkaya BU, Baker JW, Deierlein GG. Quantifying the impacts of modeling uncertainties on the seismic drift demands and collapse risk of buildings with implications on seismic design checks. *Earthquake Engineering & Structural Dynamics* 2016; 45(10): 1661–1683. doi: 10.1002/eqe.2740

11. O'Reilly GJ, Sullivan TJ. Quantification of modelling uncertainty in existing Italian RC frames. *Earthquake Engineering & Structural Dynamics* 2018; 47(4): 1054–1074. doi: 10.1002/eqe.3005

12. Der Kiureghian A, Ditlevsen O. Aleatory or epistemic? Does it matter?. *Structural Safety* 2009; 31(2): 105–112. doi: 10.1016/j.strusafe.2008.06.020

13. Bradley B. A critical examination of seismic response uncertainty analysis in earthquake engineering. *Earthquake Engineering & Structural Dynamics* 2013; 42(11): 1717–1729. 5doi: 10.1002/eqe.2331

14. ATC ATC. , ed.*FEMA P58: Seismic Performance Assessment of Buildings - Methodology*. 1. Federal Emergency Management Agency. 1 ed. 2012.

15. Terzic V, Schoettler MJ, Restrepo JI, Mahin SA. Concrete Column Blind Prediction Contest 2010: Outcomes and Observations. PEER Report 2015/01, Pacific Earthquake Engineering Reserach Center; 2015.

16. Ebrahimian H, Astroza R, Conte J, Hutchinson T. Pretest Nonlinear Finite-Element Modeling and Response Simulation of a Full-Scale 5-Story Reinforced Concrete Building Tested on the NEES-UCSD Shake Table. *Journal of Structural Engineering* 2018; 144(3): 04018009. 4doi: 10.1061/(ASCE)ST.1943-541X.0001963

17. Moaveni B, Barbosa AR, Conte JP, Hemez FM. Uncertainty analysis of system identification results obtained for a seven-story building slice tested on the UCSD-NEES shake table: Uncertainty Analysis of System Identification Results. *Structural Control and Health Monitoring* 2014; 21(4): 466–483. doi: 10.1002/stc.1577

18. Ebrahimian H, Astroza R, Conte JP, Papadimitriou C. Bayesian optimal estimation for output-only nonlinear system and damage identification of civil structures. *Structural Control and Health Monitoring* 2018; 25(4): e2128. doi: 10.1002/stc.2128

19. Astroza R, Alessandri A, Conte JP. A dual adaptive filtering approach for nonlinear finite element model updating accounting for modeling uncertainty. *Mechanical Systems and Signal Processing* 2019; 115: 782–800. 4doi: 10.1016/j.ymssp.2018.06.014

20. Li Y, Astroza R, Conte JP, Soto P. Nonlinear FE model updating and reconstruction of the response of an instrumented seismic isolated bridge to the 2010 Maule Chile earthquake. *Earthquake Engineering & Structural Dynamics* 2017; 46(15): 2699–2716. 3doi: 10.1002/eqe.2925

21. Astroza R, Alessandri A. Effects of model uncertainty in nonlinear structural finite element model updating by numerical simulation of building structures. *Structural Control and Health Monitoring* 2019; 26(3): e2297. 4doi: 10.1002/stc.2297

22. Li C, Mahadevan S. Role of calibration, validation, and relevance in multi-level uncertainty integration. *Reliability Engineering & System Safety* 2016; 148: 32–43. 5doi: 10.1016/j.ress.2015.11.013

23. Absi GN, Mahadevan S. Multi-fidelity approach to dynamics model calibration. *Mechanical Systems and Signal Processing* 2016; 68-69: 189–206. doi: 10.1016/j.ymssp.2015.07.019

24. Kersting RA, Fahnestock LA, Lopez WA. Seismic design of steel buckling-restrained braced frames: a guide for practicing engineers. Tech. Rep. NIST GCR 15-917-34, National Institute of Standards and Technology; Gaithersburg, MD: 2016. 4.

25. Fahnestock LA, Sause R, Ricles JM. Seismic Response and Performance of Buckling-Restrained Braced Frames. *Journal of Structural Engineering* 2007; 133(9): 1195–1204. doi: 10.1061/(ASCE)0733-9445(2007)133:9(1195)

26. Tremblay R, Bolduc P, Neville R, DeVall R. Seismic testing and performance of buckling-restrained bracing systems. *Canadian Journal of Civil Engineering* 2006; 33(2): 183–198. doi: 10.1139/l05-103

27. Black C, Makris N, Aiken I. Component Testing, Stability Analysis and Characterization of Buckling-Restrained Unbonded Braces. PEER Report 2002/08, Pacific Earthquake Engineering Reserach Center; 2002.

28. Zona A, Dall'Asta A. Elastoplastic model for steel buckling-restrained braces. *Journal of Constructional Steel Research* 2012; 68(1): 118–125. doi: 10.1016/j.jcsr.2011.07.017

29. Chisari C, Francavilla A, Latour M, Piluso V, Rizzano G, Amadio C. Critical issues in parameter calibration of cyclic models for steel members. *Engineering Structures* 2017; 132: 123–138. doi: 10.1016/j.engstruct.2016.11.030

30. Rossi PP. Importance of Isotropic Hardening in the Modeling of Buckling Restrained Braces. *Journal of Structural Engineering* 2015; 141(4): 04014124. doi: 10.1061/(ASCE)ST.1943-541X.0001031

31. Zsarnóczay A, Vigh LG. Eurocode conforming design of BRBF – Part II: Design procedure evaluation. *Journal of Constructional Steel Research* 2017; 135: 253–264. doi: 10.1016/j.jcsr.2017.04.013

32. Vigh LG, Zsarnóczay A, Balogh T. Eurocode conforming design of BRBF – Part I: Proposal for codification. *Journal of Constructional Steel Research* 2017; 135: 265–276. doi: 10.1016/j.jcsr.2017.04.010

33. Zsarnóczay A. *Experimental and Numerical Investigation of Buckling Restrained Braced Frames for Eurocode Conform Design Procedure Development, Ph.D. Dissertation*. Budapest University of Technology and Economics . 2013.

34. Asgarian B, Shokrgozar H. BRBF response modification factor. *Journal of Constructional Steel Research* 2009; 65(2): 290–298. doi: 10.1016/j.jcsr.2008.08.002

35. Kim J, Park J, Kim SD. Seismic behavior factors of buckling-restrained braced frames. *Structural Engineering and Mechanics* 2009; 33(3): 261–284. doi: 10.12989/sem.2009.33.3.261

36. Steel Construction AISC oAI., ed.*ANSI/AISC 341-10 Seismic Provisions for Structural Steel Buildings*. Chicago: AISC . 2010.

37. Standardization CEN fEC., ed.*EN 15129: Anti-seismic devices*. European Committee for Standardization . 2009.

38. Mazzolani FM, Corte GD, D'Aniello M. Experimental Analysis of Steel Dissipative Bracing Systems for Seismic Upgrading. *Journal of Civil Engineering and Management* 2009; 15(1): 7–19. doi: 10.3846/1392-3730.2009.15.7-19

39. Miller DJ, Fahnestock LA, Eatherton MR. Development and experimental validation of a nickel–titanium shape memory alloy self-centering buckling-restrained brace. *Engineering Structures* 2012; 40: 288–298. doi: 10.1016/j.engstruct.2012.02.037

40. Mergos PE, Beyer K. Loading protocols for European regions of low to moderate seismicity. *Bulletin of Earthquake Engineering* 2014; 12(6): 2507–2530. doi: 10.1007/s10518-014-9603-3

41. Krawinkler H, Parisi F, Ibarra L, Ayoub A, Medina R. Development of a testing protocol for woodframe structures. CUREE publication W-02, Consortium of Universities for Research in Earthquake Engineering; 2000.

42. Wang CL, Usami T, Funayama J. Evaluating the influence of stoppers on the low-cycle fatigue properties of high-performance buckling-restrained braces. *Engineering Structures* 2012; 41: 167–176. doi: 10.1016/j.engstruct.2012.03.040

43. Richards PW, Uang CM. Testing Protocol for Short Links in Eccentrically Braced Frames. *Journal of Structural Engineering* 2006; 132(8): 1183–1191. doi: 10.1061/(ASCE)0733-9445(2006)132:8(1183)

44. Zsarnóczay A, Dunai L. Type Testing of Buckling Restrained Braces according to EN 15129 - 600 BCE and 825 BCE test report. tech. rep., Department of Structural Engineering, Budapest University of Technology and Economics; 2013.